Available online at www.sciencedirect.com

ScienceDirect

Physics Procedia 3 (2010) 1133–1137

Physics Procedia

www.elsevier.com/locate/procedia

14th International Conference on Narrow Gap Semiconductor and Systems

Unusual Diamagnetism in Semiconductor Nano-Objects

L. M. Thu and O. Voskoboynikov*

National ChiaoTung University, 1001 Ta Hsueh Rd., Hsinchu 300, Taiwan, R.O.C

Abstract

We theoretically consider the diamagnetic response of an *InAs/GaAs* asymmetrical nano-ring and asymmetrical quantum dot molecule when external magnetic field is applied in the system's growth directions. We use the effective one-electronic-band Hamiltonian (energy-position-dependent electron effective mass and g-factor approximation) with smooth full three-dimensional confinement potentials mapping actual strain and material content in those nano-objects. This approach allows us to simulate and study physical properties of semiconductor nano-objects within a wide range of change in geometry and parameters. Although the geometries of the systems investigated are very different, we found for both systems a similar magnetic response. At low temperature the single electron differential magnetic susceptibility has a positive peak and with temperature increasing the peak remain Lorenzt-like shaped and gradually disappear.

Keyword: Quantum dots; Nano rings; Diamagetism.

1. Introduction

The demand for new nano-based semiconductor devices stimulates the development of novel nano-structured metamaterials [1]. Possible urgent implementations in this field are large scale quantum computation, metamaterials with the negative refracting index in optical range, static and dynamic artificial magnetism, etc. The metamaterial properties derive from properties of nano-components (nano-objects) made from the conventional semiconductors. Recent advance in semiconductor nanotechnology makes it possible to design and study in detail different kinds of semiconductor nano-objects and fabricate artificial semiconductor nano-structure such as quantum dots and nano-rings, etc. Those nano-objects are nano-sized semiconductor structures resembling artificial atoms and their magnetic properties attracted much interest in recent decade [2-10]. We use a computational method which allows us three dimensionally to map realistic geometry, strain and material composition of semiconductor nano objects (known from experiments) on smooth three dimensional potential's and parameter's profiles for electrons confined in the objects. Therefore we are able to compare some physical properties of nano-objects with very different

* Corresponding author. Tel.: +886-3-5712121-54174; fax: +886-3-5724361.
E-mail address: vam@faculty.nctu.edu.tw.

doi:10.1016/j.phpro.2010.01.151

geometries within on approach. In this theoretical study we consider and compare diamagnetic response in two types of the nano-objects: asymmetrical nano-rings (ANR) and asymmetrical quantum dot molecules (AQDM).

2. Method description

To simulate *InAs/GaAs* nano-objects we use the effective one-electronic-band Hamiltonian (energy and position-dependent electron effective mass and g-factor approximation) [8,11]:

$$\hat{H} = \frac{1}{2}\prod_{\mathbf{r}} \frac{1}{m(E,\mathbf{r})} \prod_{\mathbf{r}} + V(\mathbf{r}) + \frac{\mu_B}{2} g(E,\mathbf{r})\boldsymbol{\sigma}.\mathbf{B}, \tag{1}$$

where: $\prod_{\mathbf{r}} = -i\hbar\nabla_{\mathbf{r}} + e\mathbf{A}(\mathbf{r})$ is the electronic momentum operator, $\nabla_{\mathbf{r}}$ is the spatial gradient, $\mathbf{A}(\mathbf{r})$ is the vector potential of the magnetic field $\mathbf{B}$ = curl $\mathbf{A}(\mathbf{r})$, $V(\mathbf{r})$ is the confinement potential, $\boldsymbol{\sigma}$ is the vector of the Pauli matrices, μ_B is the Bohr magneton, m_0 and e stand for the free electron elementary mass and charge, $m(E, \mathbf{r})$ is the energy (E) and position ($\mathbf{r} = \{x, y, z\}$) dependent electron effective mass:

$$\frac{1}{m(E,\mathbf{r})} = \frac{1}{m_b(\mathbf{r})}\left[\frac{2}{E_g(\mathbf{r})} + \frac{1}{E_g(\mathbf{r}) + \Delta(\mathbf{r})}\right]^{-1}\left[\frac{2}{E + E_g(\mathbf{r}) - V(\mathbf{r})} + \frac{1}{E + E_g(\mathbf{r}) - V(\mathbf{r}) + \Delta(\mathbf{r})}\right], \tag{2}$$

and $g(E,\mathbf{r})$ is Landé factor:

$$g(E,\mathbf{r}) = 2\left\{1 - \frac{m_0}{m(E,\mathbf{r})} \cdot \frac{\Delta(\mathbf{r})}{3[E + E_g(\mathbf{r}) - V(\mathbf{r})] + 2\Delta(\mathbf{r})}\right\}, \tag{3}$$

where $m_b(\mathbf{r})$ is the effective mass at the bottom of the conducting band, $E_g(\mathbf{r})$ is the position dependent band gap and $\Delta(\mathbf{r})$ is the spin-orbit interaction splitting. $V(\mathbf{r})$ is smooth full three-dimensional confinement potential:

$$V(x,y,z) = V_{\max} - \frac{\Delta E_C}{4}\left[1 + \tanh\left(\frac{z - z_0}{a}\right)\right] \cdot \left[1 - \tanh\left(\frac{z - h(x,y)}{a}\right)\right] \tag{5}$$

mapping the actual strain and *In* content in the nano-objects embedded in the *GaAs* matrix. In Equation 5: $V_{\max}$ is the maximum value of the potential (outside of the object), $\Delta E_C = V_{\max} - V_{\min}$ is the electronic band offset in the system, and $V_{\min}$ is the minimum value of the potential (inside the object), the slope of potential and the range of the potential change at the boundaries of the object is controlled by the parameter a (the potential describes the hard wall confinement when $a \to 0$), $h(x, y)$ is function presents the height of the object in the z direction (the system's growth direction). Using analysis of the experiment structural and composition information obtained from AFM (atomic force microscopy) and XSTM (cross-section scanning tunneling microscopy) measurement, the function $h(x,y)$ can be readily discovered and even analytically approximated for most of the objects. For the *InAs/GaAs* ANR (see Fig.1) the height of the ring $h_r(x, y)$ can be obtained from the experimental fitting [10,12,13]:

$$\begin{aligned} h_r(x,y) &= h_0 + \frac{\left[h_M\left(1 + \xi\frac{x^2 - y^2}{x^2 + y^2}\right) - h_0\right]\gamma_0^2}{R^2} \cdot \frac{R^2 - \left(\sqrt{x^2 + y^2} - R\right)^2}{\left(\sqrt{x^2 + y^2} - R\right)^2 + \gamma_0^2}, \qquad \sqrt{x^2 + y^2} \le R \\ h_r(x,y) &= h_\infty + \frac{\left[h_M\left(1 + \xi\frac{x^2 - y^2}{x^2 + y^2}\right) - h_\infty\right]\gamma_0^2}{\left(\sqrt{x^2 + y^2} - R\right)^2 + \gamma_0^2}, \qquad \sqrt{x^2 + y^2} \ge R \end{aligned} \tag{6}$$

where h_0, h_M, h_∞ stand correspondingly for the height at the center of the ring, at the rim of the ring (where $x^2+y^2=R^2$), and far away from the center of the ring; γ_0, γ_∞ respectively determine the inner and outer slope near the rim. The parameter ξ defines the anisotropy of the ring in the (x, y) plane.

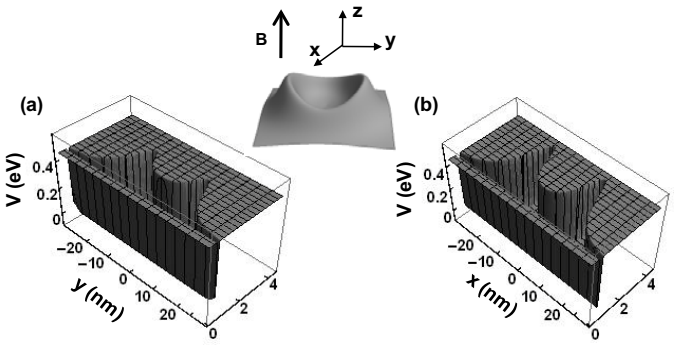

Fig. 1. Projections of the confinement potential on (a) (x =5 nm,y,z) and (b) (x, y =5 nm,z) planes.

For both quantum dots in the *InAs/GaAs* ADQM (see Fig. 2) we adopt the lens-shaped geometry from [14,15] and the height of the each dot $h_d(x, y)$ can be presented as

$$h_d(x,y) = \sqrt{R_u^2 - (x^2 - y^2)} - \sqrt{R_u^2 - R_b^2} \tag{7}$$

where R_u is the radius of the upper circle and R_b is the base radius of the dot.

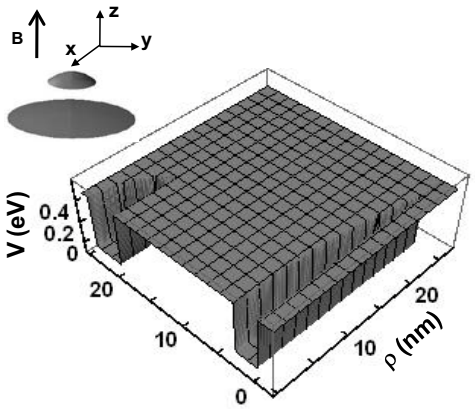

Fig. 2. Confinement potential of double dot system.

The potential from (5) is used to define the mapping function

$$M(x,y,z) = \frac{V_{\max} - V(x,y,z)}{\Delta E_C} \tag{8}$$

The mapping function reproduces experimental information about geometry (shape) and position dependent composition of the object. Using $M(x,y,z)$ we model the position dependent band gap $E_g(x,y,z)$, spin-orbit interaction splitting $\Delta(x,y,z)$, and the effective mass at the bottom of the conducting band $m_b(x,y,z)$:

$$\begin{aligned} E_g(x,y,z) &= E_{gin} M(x,y,z) + E_{gout}[1 - M(x,y,z)] \\ \Delta(x,y,z) &= \Delta_{in} M(x,y,z) + \Delta_{out}[1 - M(x,y,z)] \\ m_b(x,y,z) &= m_{bin} M(x,y,z) + m_{bout}[1 - M(x,y,z)] \end{aligned} \tag{9}$$

To determine the single electron magnetic response of an isolated nano-object we calculate the total energy of the electron confined in the nano-object in the presence of the external magnetic field. The magnetization M and different magnetic susceptibility (DMS) χ of the systems are defined by

$$M = \sum_n \left(-\frac{\partial E_n}{\partial B} \right) f(E_n - \mu), \; \chi = \frac{\partial M}{\partial B}, \tag{10}$$

where $f(E)$ is the Fermi-Dirac distribution function, and μ is the chemical potential of the system determined from the number of electrons in the nano-object by the following equation

$$N = \sum_n f(E_n - \mu), \tag{11}$$

3. Simulation Results and Discussion

To simulate diamagnetic response in the ANR and ADQM we take realistic semiconductor parameters for *InAs/GaAs* nano-structures with complex strained composition according to [15-17]: E_{gin} = 0.86eV, E_{gout} = 1.519, Δ_{in} = 0.37, Δ_{out} = 0.341, m_{bin} = 0.044 m_0, m_{bout} = 0.067 m_0, V_{min} = 0, V_{max} = ΔE_C = 0.474eV. We also accept the geometry parameters for ANR from [12,13] and for ADQM from [15,16] . The energy states and wave functions of the electrons confined in the nano-objects are found by the nonlinear iterative method [18] using the Comsol Multiphysics package (www.comsol.com). Then the magnetic response of single electron ANR and ADQM is calculated (see Fig. 3).

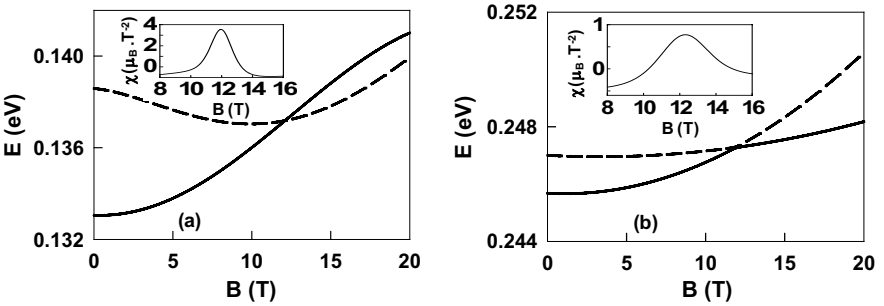

Fig. 3. Magnetization of single electron of (a) ANR and (b) ADQM at temperature T =1.2K

For both systems at zero temperature the single electron DMS has a positive peak near 12T. With temperature increasing the peaks remain Lorentz-like shaped and gradually disappear. And for both systems considered the peaks are results of the convergence of two lowest energy levels when the magnetic field increases. But for ANR the wave functions have different symmetry and levels *cross*. At the same time, for ADQM the wave functions have the same symmetry and the levels *anticross*. Although the topology of the systems is different the convergence leads to about the same unusual diamagnetic response for both. We can assume that this unusual diamagnetic response can be observed in nano objects where the lowest energy states are close enough and they converge when magnetic field is applied to the system.

4. Conclusion

It follows from this theoretical study that our method can efficiently and economically reproduces physical properties of semiconductor nano-objects of very different geometries and material parameters. The diamagnetic response following the semiconductor nano-objects geometry can be very unusual and even reverse the sign. Experimental investigations of the diamagnetic response of nano-objects made from conventional semiconductors will yield interesting results and can be useful for further fabrication of metamaterials with principally new magnetic properties.

Acknowledgment

This work is supported by the National Science Council of the Republic of China under Contracts No. No. 97-2112-M-009-012-MY3 and NSC 97-2120-M-009-004 and by the Aim for the Top University Plan of the National Chiao Tung University and Ministry of Education of Taiwan, R.O.C.

References

1. M. Shalaev, Nature Photonic 1 (2006) 41.
2. S. M. Reiman and M. Manninen, Rev. Mod. Phys. 74 (2006) 1283.
3. J. Stangl, V. Holý, and G. Bauer, Rev. Mod. Phys. 76 (2005) 725.
4. F. Boxberg and J. Tulkki, Rep. Prog. Phys. 70 (2007) 1425.
5. R. Hanson, L. P. Kouwenhoven, J. R. Petta, S. Tarucha, and L. M. K. Vandersypen, Rev. Mod. Phys. 79, 1217 (2007).
6. J. M. Garsía, G. Medeiros-Ribeiro, K. Schmidt, T. Ngo, J. L. Feng, A. Lorke, J. Kotthaus, and P. M. Petroff, Appl. Phys. Lett. 71 (1997) 2014.
7. A. Lorke, R. J. Luyken, A. O. Govorov, J. P. Kotthaus, J. M. Garcia and P. M. Petroff, Phys. Rev. Lett. 84 (2000) 2223.
8. O. Voskoboynikov, Y. Li, H. M. Lu, C. F. Shih, and C. P. Lee, Phys. Rev. B 66 (2002) 155306.
9. J. I. Climente, J. Planelles, and J. L. Movilla, Phys. Rev. B 70, 081301 (2004).
10. N. A. J. M. Kleemans, I. M. A. Bominaar-Silkens, V. M. Fomin, V. N. Gladilin, D. Granados, A. G. Taboada, J. M. García, P. Offermans, U. Zeitler, P. C. M. Christianen, J. C. Maan, J. T. Devreese, and P. M. Koenraad, Phys. Rev. Lett. 99 (2007) 146808.
11. G. Bastard, Wave Mechanics Applied to Semiconductor Heterostructures, Les Edition de Physique, Les Ulis, 1990.
12. P. Offermans, P. M. Koenraad, J. H. Wolter, D. Granados, J. M. García, V. M. Fomin, V. N. Gladilin, and J. T. Devreese, Appl. Phys. Lett. 87 (2005) 131902.
13. V. M. Fomin, V. N. Gladilin, S. N. Klimin, J. T. Devreese, N. A. J. M. Kleemans, and P. M. Koenraad, Phys. Rev. B 76 (2007) 235320.
14. D. M. Bruls, J. W. A. M. Vugs, P. M. Koenraad, M. S. Skolnock, M. Hopkinson, J. H. Wolter, Appl. Phys. A 72 (2001) S205.
15. O. Voskoboynikov, Phys. Rev. B 78 (2008) 113310.
16. C. E. Pryor and M. E. Pistol, Phys, Rev. B 72 (2005) 205311.
17. I. Vurgaman, J. R. Meyer, and L. R. Ram-Mohan, J. Appl. Phys. 89 (2001) 5815.
18. Y. M. Li , O. Voskoboynikov, C. P. Lee, and S. M. Sze, Comput. Phys. Commun. 141 (2001) 66.